Published in final edited form as:
J Clin Immunol. 2012 June ; 32(3): 551–564. doi:10.1007/s10875-012-9663-6.

B-cell tolerance defects in the B6.Aec1/2 mouse model of Sjögren's syndrome

Wenzhao Meng,
Department of Pathology and Laboratory Medicine, Perelman School of Medicine, University of Pennsylvania, Philadelphia, PA 19104, USA

Yongmei Li,
Section of Rheumatology, Department of Medicine, Temple University School of Medicine, Philadelphia, PA 19140, USA

Emily Xue,
Department of Pathology and Laboratory Medicine, Perelman School of Medicine, University of Pennsylvania, Philadelphia, PA 19104, USA

Minoru Satoh,
Division of Rheumatology and Clinical Immunology, Department of Medicine, University of Florida, Gainesville, FL 32610, USA

Ammon B. Peck,
Department of Pathology, Immunology and Laboratory Medicine, University of Florida College of Medicine, Gainesville, FL 32610, USA

Philip L. Cohen,
Section of Rheumatology, Department of Medicine, Temple University School of Medicine, Philadelphia, PA 19140, USA

Robert A. Eisenberg, and
Division of Rheumatology, Department of Medicine, Perelman School of Medicine, University of Pennsylvania, Philadelphia, PA 19104, USA

Eline T. Luning Prak, MD, PhD
Department of Pathology and Laboratory Medicine, Perelman School of Medicine, University of Pennsylvania, 405B StellarChance Labs, 422 curie Blvd., Philadelphia, PA 19104, tel (215) 746-5768, fax (215) 573-6317

Eline T. Luning Prak: luning@mail.med.upenn.edu

Abstract

Purpose—Primary Sjögren's syndrome (SjS) is an autoimmune disorder characterized by lymphocytic infiltration of the salivary and lacrimal glands, B-cell clonal expansions and an increased risk of lymphoma. In order to understand the role of B cells in this disorder, the antibody repertoire and B-cell maturation were studied in a mouse model of SjS called B6.Aec1/2.

Methods—B6.Aec1/2 serum was analyzed for (auto)antibodies by ELISA and immunoprecipitation, B-cell development by flow cytometry, antibody gene rearrangements by CDR3 spectratyping and quantitative PCR. In order to test the functional consequences of the observed defects, B6.Aec1/2 mice were crossed with anti-dsDNA antibody heavy chain knock-in mice (B6.56R).

Results—B6.Aec1/2 mice exhibit B-cell clonal expansions, have altered serum immunoglobulin levels and spontaneously produce multireactive autoantibodies. B6.Aec1/2 mice also have decreased numbers of bone marrow pre-B cells and decreased frequencies of kappa light chain

gene deletion. These findings suggest that B6.Aec1/2 mice have a defective early B-cell tolerance checkpoint. B6.56R.Aec1/2 mice unexpectedly had lower anti-dsDNA antibody levels than B6.56R mice and less salivary gland infiltration than B6.Aec1/2 mice.

Conclusions—These data suggest that the early tolerance checkpoint defect in B6.Aec1/2 mice is not sufficient to promulgate disease in mice with pre-formed autoantibodies, such as B6.56R. Rather, B6.Aec1/2 mice may require a diverse B-cell repertoire for efficient T-B-cell collaboration and disease propagation. These findings imply that therapies aimed at reducing B-cell diversity or T-B interactions may be helpful in treating SjS.

Keywords

Sjögren's syndrome; B cell; autoantibody; receptor editing

Introduction

Primary Sjögren's syndrome (SjS) is a chronic autoimmune disease featuring infiltration of exocrine glands with lymphocytes. SjS patients, particularly those with the primary syndrome, frequently produce a variety of autoantibodies including anti-nuclear antibodies, rheumatoid factors and anti-muscarinic receptor antibodies, as well as the diagnostic antibodies directed against the ribonuclear proteins SSA/Ro and SSB/La (1–6). This disease exhibits a strong gender bias, with females outnumbering males about 9:1 (7). SjS is an important clinical problem without effective treatment (8, 9). Although the cause of SjS remains unidentified, both T cells and B cells and their products seem to be important for its pathogenesis. CD4+ T cells comprise the majority of mononuclear infiltrates in salivary glands, and CD4+ T cell expansion has been observed in glands, spleen and lymph nodes (10–12). Yet, glandular tissue also contains significant numbers of B cells and some CD8+ T cells (10–12).

B cells appear to play several roles in the development of SjS: by accumulating in involved tissues, by secreting autoantibodies, and possibly by participating in the immune and inflammatory response, leading to glandular failure and destructive infiltration of the glandular parenchyma (13–15). SjS B cells have an activated phenotype and proliferate locally in the salivary glands, as reflected in their oligoclonality in the minor salivary glands of SjS patients (16–19). The B-cell stimulatory factor BAFF may stimulate B cells in SjS, as it circulates in increased levels and it is produced locally in salivary glands by infiltrating cells (20). Furthermore, the overexpression of BAFF in transgenic mouse models produces a Sjögren's-like syndrome that develops in older animals, with features that are also seen in human SjS, including xerostomia, lymphocytic infiltrates in exocrine glands, marginal zone B-cell expansion and an increased frequency of B-cell lymphomas (21). In human SjS, B-cell hyperactivity is also manifested through the high prevalence (particularly in patients with primary SjS) of hypergammaglobulinemia and autoantibodies (4, 6, 22). SjS patients are also at significantly greater risk (40–100 times higher than the general population) for developing malignant B-cell lymphoma (19, 23, 24). B-cell lines derived from SjS patients show increased DNA-dependent protein kinase activity, along with increased apoptosis and cell-cycle arrest (25). It has been suggested that abnormal retention of immunoglobulin transcripts preceding switch rearrangement may signify abnormal peripheral B-cell memory in SjS (26, 27).

To study the roles of B cells in SjS pathogenesis, we herein evaluate B-cell development and antibody repertoire in a mouse model of SjS called B6.Aec1/2. Non-obese diabetic mice (NOD) develop a SjS-like syndrome, with salivary and lacrimal gland lymphocyte infiltration and xerostomia (28). B6.Aec1/2 mice have two NOD-derived genetic intervals (Idd-3 and Idd-5) and have been bred onto the C57BL/6 background (B6) (29). These NOD

intervals have been shown to be responsible for a Sjögren's syndrome-like phenotype that includes salivary and lacrimal gland inflammation, decreased tear and saliva production and anti-nuclear antibodies (ANA) (30, 31). The onset of Sjögren's syndrome-like features is dependent upon the complement component C3, suggesting that B cells are involved in disease pathogenesis, but the nature of the B-cell defect(s) and potential defects in censoring of the autoantibody repertoire have not been defined. The B6.Aec1/2 model is useful for the genetic analysis of antibody repertoire, because the B6 genome has been sequenced, including the IgH and IgL loci (32–34); because the antibody repertoire has been studied previously in B6; and because there are immunoglobulin transgenic mice that are bred onto the B6 background, such as B6.56R. The B6.56R mouse has a high-affinity anti-dsDNA heavy chain knocked into the heavy chain locus (35). The autoantibody repertoire and B-cell tolerance mechanisms have been extensively characterized in B6.56R mice (36–38).

Thus, the B6.Aec1/2 mouse provides the opportunity to study B-cell tolerance checkpoints through the analysis of mice with different B-cell repertoires, ranging from diverse (B6 and B6.Aec1/2) to highly restricted and autoimmune-prone (B6.56R and B6.56R.Aec1/2), all on the well-characterized B6 background. The comparison of B-cell development and repertoire between B6 and B6.Aec1/2 provides insights into alterations in the B-cell compartment that are due to the presence of the Aec1/2 NOD intervals. By extending the comparison to B6.56R and B6.56R.Aec1/2, we can evaluate how the Aec1/2 NOD intervals influence B-cell tolerance in the setting of limited antibody diversity with a known autoreactive antibody. If the Aec1/2 NOD intervals relax B-cell selection stringency or promote lymphocytic infiltration in the setting of autoantibody production, then we predict the development of significantly worse disease in B6.56R.Aec1/2 mice than in either B6.56R or B6.Aec1/2. Unexpectedly, we found less salivary gland inflammation in B6.56R.Aec1/2 mice compared to B6.Aec1/2 mice. We propose that autoimmunity in the B6.Aec1/2 model requires that autoantibodies of particular specificities need to be generated and that pathogenic B-cell clones harboring these autoantibodies are more likely to arise in the setting of a diverse antibody repertoire.

Methods

Mice

B6.Aec1/2 mice were generated at the University of Florida and transferred to the University of Pennsylvania, where they were crossed with B6.56R mice to generate B6.56R.Aec1/2 mice. C57Bl6/J (hereafter B6), B6.56R, B6.Aec1/2 and B6.56R.Aec1/2 mice were maintained in the Perelman School of Medicine animal colony at the University of Pennsylvania under an Institutional Animal Care and Use Committee-approved protocol.

Mouse genotyping

Mouse genotypes were determined by PCR amplification of genomic DNA from tail biopsies. Each 20-μl PCR contained 50 ng genomic DNA, 2μl PCR buffer (AmpliTaq Gold 10× PCR buffer I with 15 mM $MgCl_2$; Roche Applied Sciences, Indianapolis, IN), 0.2 mM of each dNTP (dATP, DTTP, dGTP, and dCTP; Promega, Madison, WI), 0.6 μM of each primer, and 1U of DNA polymerase (AmpliTaq Gold; Roche Applied Sciences). The cycling conditions were 10 min at 94°C, followed by 40 cycles of 94°C for 30 s, T_a (see specific primer combinations) for 30 s, and 72°C for 30 s, followed by 20 min at 72°C. The 56R genotyping PCR uses the V_H3H9 LD and CDR3 primers (39) with T_a of 58°C, and the wild-type allele uses J_H1 upstream primers (40) with T_a at 60°C. PCR assays were used to identify the Idd3 and Idd5 intervals as described previously (30, 31, 41). Idd3 (Aec1) is located on Chromosome 3 and microsatellite markers D3Mit132 and Tshb were used to

identify this interval. Idd5 (Aec2) is located on Chromosome 1 and microsatellite markers D1Mit005 and D1Mit15 were used to identify this interval.

Flow Cytometry

Cell suspensions from 3–4 month old mice were prepared from femurs, tibias, and spleens in FACS buffer (PBS, 0.5% BSA, 0.01% NaN_3, 1 mM EDTA) after red blood cell lysis (ACK Lysing Buffer; BioWhittaker, Walkersville, MD). All antibodies were purchased from eBioscience (San Diego, CA), BD Biosciences (San Jose, CA) and BioLegend (San Diego, CA). The following antibody-fluorophore combinations were used to resolve BM subsets: FITC anti–heat-stable antigen (30F1), PE anti-CD43 (S7), PE-Cy7 anti-IgM (II/41), PE-Cy5.5 anti-CD19 (1D3), APC anti-CD93 (AA4.1), APC-AF750 anti-B220 (RA3-6B2), Pacific Blue anti-IgD (11–26). BM B-cell fractions are defined as follows, based upon the scheme by Hardy (42): Fr.A-C′ ($B220^+CD19^+CD43^+$), Fr.D ($B220^+CD43^-IgM^-IgD^-CD93^+$), Fr.E ($B220^+CD43^-IgM^+IgD^-CD93^+$) and Fr.F ($B220^+CD43^-IgM^{dim/+}IgD^+CD93^-$). The following antibodies were used to resolve splenic B-cell subsets: FITC anti-IgM (II/41), PE anti-CD21 (7G6), APC anti-CD93 (AA4.1) and APC-AF750 anti-B220 (RA3-6B2). Splenic B-cell subsets were defined as follows: Transitional ($B220^+CD93^+$), Follicular ($B220^+CD93^-IgM^{dim}CD21^{dim}$) and Marginal zone ($B220^+CD93^-IgM^{bri}CD21^{bri}$). For all flow sorts, dead cells were first eliminated by DAPI staining and cell doublets/aggregates by pulse width gating. FACS analysis and sorting were performed on the LSR II and FACSAria cytometers, respectively, (BD Bioscience, San Jose, CA) in the University of Pennsylvania Flow Cytometry core facility. Flow cytometry data were analyzed using FlowJo software (version7.5.5, Treestar Inc., Ashland, OR). Absolute B-cell counts were calculated by multiplying the number of live bone marrow B cells (counted on a hemocytometer following trypan blue staining) by the CD19+ lymphocyte fraction. Absolute B-cell counts using this method are variable and one of the largest sources of variability in the measurement comes from non-uniform bone marrow harvests.

Histology and Confocal Microscopy

Freshly isolated tissues were fixed in 10% phosphate-buffered formalin. Each tissue was embedded in paraffin and 5-μm sections were stained with hematoxylin and eosin at University of Pennsylvania Histology core facility. The stained sections were viewed by light microscopy at 100× magnification. Focal inflammatory infiltrates in kidneys and submandibular salivary glands were enumerated: the number of mononuclear cell infiltrates (having more than 50 cells) in a 4 mm^2 histological section was defined as the focus score as described in reference (43). For confocal images, 5–6 μm spleen cryostat sections were prepared and stained with anti-CD4-Alexa647 (clone RM4-5 from BD Pharmingen) and anti-B220-Alexa488 as described in (44).

Hybridomas

Spontaneous hybridomas were generated from splenocytes of a 20-month old female B6.Aec1/2 mouse. Splenocytes were fused to the Sp2/0 myeloma partner in polyethylene glycol, hybridomas were selected in HA medium. Supernatants were tested for antibody production and light chain isotypes, where applicable (see ELISA section), and genomic DNA from each hybridoma was analyzed for antibody gene rearrangements. Kappa light chain genotyping PCRs were performed in a 20 l reaction containing 50 ng hybridoma genomic DNA, 2 μl PCR buffer (AmpliTaq Gold 10× PCR buffer I with 15 mM $MgCl_2$; Roche Applied Sciences, Indianapolis, IN), 0.2 mM of each dNTP (dATP, DTTP, dGTP, and dCTP; Promega, Madison, WI), 0.6 μM of forward (Vs, ref. (45)) and reverse (Jκ2 or Jκ4/5, ref. (46)) primers, and 1U of DNA polymerase (AmpliTaq Gold; Roche Applied Sciences). The cycling conditions were 10 min at 94°C, followed by 40 cycles of 94°C for 30 s, 65°C for 30 s, and 72°C for 90 s, followed by a final extension of 10 min at 72°C.

Quantitative PCR for RS rearrangements

Genomic DNA was isolated from sorted B cells using the Gentra Puregene Tissue Kit (Qiagen, Valencia, CA). Reactions contained 25–50 ng template DNA in a 20 μl reaction mix containing 10 μl LightCycler 480 Probes Master Mix (Roche Applied Sciences, Indianapolis, IN), 0.5 U LightCycler Uracil-DNA Glycosylase (Roche), 0.6 μM of forward/reverse primer and 0.12 μM of a hydrolysis probe. Cycling conditions were: 40 ° C for 10 min, 95 ° C for 10 min, followed by 60 cycles at 95 ° C for 10 s, 60 ° C for 30 s, and 72 ° C for 1 s on a Light-Cycler 480 real-time PCR system (Roche). Primers and probes were synthesized by Integrated DNA Technologies (San Jose, CA). Vκ-RS rearrangements were amplified with 5′-GGC TGC AGS TTC AGT GGC AGT GGR TCW GGR AC-3′ (reference (45)) and 5′-CTG AGC TCA ACT GCA GTC CTA-3′ primers and detected with 5′-TGG CAG CCC AGG GTG GAT CT-3′ FAM-labeled hydrolysis probe. For each sample, the intronic region of the reference control gene, β-actin, was amplified in a separate well with forward primer 5′-GAG GCT CTT TTC CAG CCT TC-3′ and reverse primer 5′-TCC ATA CCT AAG AGA AGA GTG ACA GA-3′ and detected with a Cy5-labeled hydrolysis probe 5′-AAG GTG ACA AAA CTC CTG AGG CCA-3′. The amount of Vκ-RS product in each mouse sample was normalized to the amount of β-actin product and compared with the normalized target value in wild-type C57BL/6 B220 + κ + splenocytes to determine a relative quantity (comparative C_T method). Reactions were performed in duplicate.

CDR3 Spectratyping

CDR3 spectratyping was performed to evaluate the degree of clonal expansion. Genomic DNA was isolated from spleen, purified according to the manufacturer's directions using PureGene (Qiagen, Valencia CA), and amplified using the V_H primers and conditions described in (47) except for the MOPC21 primer which is described in (48). All primers were synthesized by Integrated DNA Technologies (Coralville, IN). 2 μL of PCR product per reaction were resolved by capillary electrophoresis on an ABI 3100 analyzer (Applied Biosciences Inc., Foster City, CA). Peak scanner v. 1.0 was used to generate analyze the spectratypes (Applied Biosciences Inc.).

Antibody ELISA

Autoantibodies against dsDNA and chromatin were evaluated by ELISA as described previously in (49, 50). Three μg/ml chicken chromatin purified from chicken erythrocyte nuclei or 3 μg/ml dsDNA purified from calf thymus (Sigma Chemical Co., St. Louis, MO) were used to coat the plate. To measure the dsDNA binding, serum samples were diluted 1:8,000 and detected with alkaline phosphatase (AP) conjugated anti-IgM, anti-IgG total or anti-IgA (Southern Biotech, Birmingham, AL). To measure chromatin binding, serum samples were diluted 1:8,000 and antibodies that bound were detected using biotin conjugated anti-IgG total and AP- streptavidin. For total serum IgM, IgG and IgA, Immulon 4 HBX plates (Fisher Scientific, Pittsburgh, PA) were coated with 100 μl/well of goat anti-mouse IgM, IgG or IgA (1 μg/ml) (SouthernBiotech, Birmingham, AL). Serum samples were diluted 1:8,000. For total IgM and IgG detection in hybridomas, a similar protocol was used except that supernatant of each hybridoma was added without dilution. The Ig assay was performed as described previously (46). For the insulin ELISA, the plate was coated with 5 μg/ml bio-insulin (Sigma Chemical Co.) and detected with AP-anti-Ig total (IgG, IgM and IgA). For the LPS ELISA, the plate was coated with 10 μg/ml LPS (from *Escherichia coli* 0111:B4, Sigma Chemical Co.) and detected with AP-anti-Ig total.

Immunoprecipitation and immunoblotting

K562 (human erythroleukemia cells, ATCC CCL-243) were metabolically labeled with ^{35}S-methionine/cysteine (DuPont New England Nuclear, Boston, MA) for 14 hours. Whole cell extracts were made by sonicating cells in 0.5M NaCl, 50mM Tris pH 7.5, 2 mM EDTA and 0.3% NP40. Extracts were immunoprecipitated on protein A and protein G Sepharose beads (Pharmacia LKB Biotechnology Inc., Piscataway, NJ) that were pre-incubated with 4 μL of mouse sera as described previously (51). Immunoprecipitates were washed and size separated by SDS-PAGE (8%) and analyzed by autoradiography as described previously (52).

Statistical analysis

Analyses were performed with a two-tailed Mann–Whitney U test as indicated.

Results

It has been shown previously that B6.Aec1/2 mice produce ANA and anti-muscarinic acetylcholine type 3 autoantibodies (53). However, the full spectrum of antibody abnormalities in the B6.Aec1/2 model has not been defined. Are there global shifts in the antibody repertoire (as reflected by altered serum immunoglobulin levels) and what is the range of autoantibody specificities? Are the autoantibodies multireactive and have they undergone class switching or somatic mutation? Understanding the range and molecular features of the autoantibodies produced in the B6.Aec1/2 model may provide insights into the nature and timing of the B-cell tolerance breakdown in this mouse model of SjS.

Altered serum immunoglobulin levels in B6.Aec1/2 mice

Reasoning that patients with SjS often exhibit hypergammaglobulinemia, we began by analyzing serum immunoglobulin levels in the B6.Aec1/2 mouse model of SjS. Unexpectedly, B6.Aec1/2 mice exhibited *lower* serum IgA levels than B6 mice and similar IgM and IgG levels (Fig. 1a). This analysis was restricted to female mice because of the previously described association of disease manifestations and female sex in the Aec mouse model (54). Differences in IgA levels were still significant when male mice were included in the analysis (data not shown). IgG levels also differed slightly but significantly between B6 and B6.Aec1/2 strains when male and female mice were included in the analysis (data not shown). Serum IgM levels were significantly higher in female than in male mice in both the B6 and the B6.Aec1/2 strains whereas serum IgG and IgA levels did not differ significantly between male and female mice of either strain (data not shown). Because sicca symptoms in the B6.Aec1/2 model are also age-dependent, we stratified the data by age. Serum levels of IgG and IgA oscillated and did not show a consistent age-related trend whereas IgM increased with increasing age in B6 (Supplementary Fig. S1a). In B6.Aec1/2 mice, immunoglobulin levels did not change appreciably with age (Supplementary Fig. S1a).

Analysis of anti-dsDNA and anti-chromatin antibodies in B6 and B6.Aec1/2 mice

Sera from B6.Aec1/2 mice have previously been analyzed for ANA reactivity, but the pattern often included cytoplasmic staining (55). To clarify the autoantibody specificities in B6.Aec1/2 mice, we therefore surveyed B6 and B6.Aec1/2 sera for anti-dsDNA and anti-chromatin antibodies. Although IgM levels of anti-dsDNA were not significantly different, IgA and IgG anti-dsDNA antibodies were higher in B6.Aec1/2 mice than in B6 mice (Fig. 1b). The higher IgA anti-dsDNA levels occurred in spite of lower overall serum IgA levels in B6.Aec1/2 mice. Although the IgG anti-dsDNA antibodies were elevated in B6.Aec1/2 mice compared to B6 mice, the level of binding was very low. Anti-chromatin IgG levels were not statistically significantly different between B6 and B6.Aec1/2 mice

(Supplementary Fig. S1b, **left panel**). When the data were stratified by age, mice (of either strain) that exhibited the highest anti-chromatin titers tended to be older than 14 months of age (Supplementary Fig. S1b, **right panel**). There was no significant linear correlation between IgG anti-chromatin titers and IgG anti-dsDNA titers (data not shown). Overall, these data indicate that B6.Aec1/2 mice have elevated levels of IgA and IgG anti-dsDNA antibodies compared to B6 mice, but the levels of binding are low.

In order to test for possible autoantibodies with specificities other than DNA or chromatin (such as anti-Ro) that could account for the previously described ANA results, we next performed screening by immunoprecipitation using whole cell extracts from K562 cells (human erythroleukemia cell line, see *Materials and Methods*). This method has been used to detect murine and human autoantibodies and is ideal for screening of autoantibodies to various intracellular antigens including Ro and La, which are associated with SjS (47). Supplementary Fig. S2a shows an example of immunoprecipitation screening of sera from patients with systemic lupus erythematosus (SLE). In this assay, bands that are uniquely seen in some samples are considered to represent specific recognition by autoantibodies. In contrast to detection of various known autoantibodies in human SLE sera, none of the B6 (n = 4) or B6.Aec1/2 mice (n = 36, Supplementary Fig. S2b and S2c, not all data are shown) had anti-Ro, La, or other standard autoantibodies associated with systemic autoimmune rheumatic diseases. Although some sera immunoprecipitated unique proteins (open arrowheads), they were weak in general, and no specific proteins were repeatedly recognized by the majority B6.Aec1/2 mouse sera. In addition, immunoprecipitation of unidentified unique proteins are not uncommon in B6 mouse sera (data not shown). Thus, by immunoprecipitation there was no strong serologic evidence of autoimmunity in B6.Aec1/2. The low frequency of various autoantibodies in B6.Aec1/2 mice could be due to incomplete penetrance, sequestration of pathogenic antibodies from the circulation or it could indicate that these antibodies are formed very late in the course of the disease.

Autoantibody production and B-cell clonal expansion in old B6.Aec1/2 mice

To further characterize the autoantibody repertoire in more detail in old mice, we generated a spontaneous hybridoma panel in a 20-month old female B6.Aec1/2 mouse. Seventy clones were obtained, of which 41 expressed IgM, 5 expressed IgG, 1 expressed IgA, 3 expressed kappa L chain but not IgM, IgG or IgA, and the remainder were nonsecretors (Fig. 2a). The hybridoma panel yielded multiple clones that were multireactive, including a class-switched antibody (IgA) that bound to dsDNA, insulin and lipopolysaccharide (Table 1). Molecular analysis of hybridoma immunoglobulin heavy chain and light chain usage revealed that 44 out of the 50 antibody-secreting clones were independent, while there were 2 expanded clones (Fig. 2b). Because members of each of the two expanded clones have sequence variation, we favor the interpretation that these clones expanded *in vivo* rather than *in vitro*.

To determine if B-cell clonal expansions are a more general feature of the B6.Aec1/2 model, we analyzed the antibody repertoire using CDR3 spectratyping. During CDR3 spectratyping, the hypervariable CDR3s of antibody heavy chains are amplified using fluorescent primers and the resulting fluorescent amplicons are size separated on a sequencing capillary. The resulting spectratype plots fluorescence intensity of the PCR products as a function of the amplicon size in nucleotides. In a polyclonal B-cell repertoire, such as the one found in splenocytes from a B6 mouse, the spectratype reveals a Gaussian distribution of peaks. In contrast, in an elderly female B6.Aec1/2 mouse, clonal expansions are evident, based upon the reproducible amplification of specific CDR3 lengths in separate DNA aliquots (Fig. 2c). Analysis with additional V_H-specific primers (3609N.2 and MOPC21) also yielded reproducible products in the same mouse, suggesting that clonal expansion is a global feature of the B-cell repertoire rather than being restricted to a

particular V_H or specificity (data not shown). Older mice are known to have reduced bone marrow output and reduced B-cell numbers, but when we tested the repertoire of an aged (23-month-old) B6 mouse using the same primers, we did not see evidence of reproducible amplification products using primers for MOPC21 (Fig. 2d). Analysis with additional primers (J606.1, 7183.2, 3609N.2) also did not reveal clonal expansions (data not shown). Taken together, these data suggest that B6.Aec1/2 mice exhibit an age-dependent accumulation of autoantibody specificities and clonal expansion.

Alterations in early B-cell development and tolerance in B6.Aec1/2 mice

Because secreted antibodies represent an end-product of B-cell maturation and activation, it is not clear from the preceding data if early B-cell tolerance is broken in B6.Aec1/2 mice. Mice with early tolerance checkpoint defects will often exhibit abnormal frequencies of particular bone marrow B-cell subsets (56). To determine if early B-cell development is abnormal in B6.Aec1/2 mice, we therefore compared bone marrow B-cell subsets in B6 and B6.Aec1/2 mice. Using the maturation scheme of Hardy (42), bone marrow B cells were divided into pro-B (Fr. A–C), large pre-B (Fr. C′), small pre-B (Fr. D), naïve (Fr. E) and recirculating (Fr. F) cells. Representative flow cytometric plots for these stages are shown in Supplementary Fig. S3. The mean percentage of B cells that comprises Fr. D is significantly lower, while the proportion of Fr. F cells is significantly higher in B6.Aec1/2 mice as compared to B6 mice (Fig. 3a). The absolute number of total B cells in bone marrow was increased in B6.Aec1/2 relative to B6 mice, with Fr. F accounting for the difference (Fig. 3b).

Fr.D cells are undergoing antibody light chain gene rearrangement, and the relative size of the Fr. D compartment is often positively correlated with the extent of receptor editing (56, 57). The decreased frequency of Fr. D cells in B6.Aec1/2 mice therefore suggested the possibility of reduced receptor editing, with relaxed selection at the pre-B to naïve B-cell transition, which is in fact observed in the parental NOD mouse (58). To test the level of receptor editing in Fr. D of B6.Aec1/2 mice, we measured the frequency of kappa light chain gene deletion using a quantitative PCR assay for RS deletion (58). RS is a non-coding sequence, located approximately 25 kb downstream of C which can participate in RAG-mediated rearrangement (59, 60). When Vκ genes rearrange to RS, Cκ is either deleted or inverted, resulting in inactivation of the kappa locus. Unlike other measures of receptor editing such as lambda light chain or Jκ skewing, the frequency of RS rearrangement is unaffected by specificity of the RS rearrangement product, because the Vκ-RS rearrangement is non-functional. Rather, the frequency of RS rearrangement is an unselected indicator of the extent of light chain rearrangement: B cells with very few rearrangements will have low frequencies of RS rearrangement, whereas B cells that have undergone extensive rearrangement (receptor editing) will have high frequencies of RS rearrangement. Based upon the reduced fraction of BM B cells in Fr. D, we expect this subset to show a decreased frequency of RS rearrangement (Fig. 3c). The RS data suggest that B6.Aec1/2 mice have decreased receptor editing and/or decreased residence time in the Fr.D compartment, consistent with a pre-B to naïve B-cell checkpoint defect, similar to the parental NOD strain (58).

Analysis of editing and B cell selection in B6.56R.Aec1/2 mice

To determine the functional consequences of the alterations in B-cell development and receptor editing in B6.Aec1/2 mice, we crossed the Aec1/2 intervals onto the B6.56R model. The 56R heavy chain, in combination with nearly all light chains, produces high affinity anti-dsDNA antibodies that are negatively selected on the B6 background. Only 56R+ B cells that harbor one of a handful of “editor” light chains (Vκ21D, Vκ38c, Vκ20, lambda X) survive (35, 61, 62). By crossing the Aec1/2 intervals onto the B6.56R background, we can

therefore determine if alterations in B-cell development or editing alter the B-cell repertoire and the stringency of light chain selection.

We first analyzed the B subsets in BM and found the same trend in B6.56R and B6.56r.Aec1/2 mice as in B6.Aec1/2 and B6 mice. The percent of Fr.D B cells was lower in B6.56R.Aec1/2 mice than in B6.56R mice, while that of Fr.F B cells was significantly higher (Fig. 4a). Fr. E was not significantly different in B6.56R compared to B6.56R.Aec1/2 mice (Fig. 4a). We also analyzed the RS rearrangement frequency which was not significantly different between B6.56R.Aec1/2 and B6.56R mice, but both of these strains of mice had higher RS levels than B6.Aec1/2 mice (Fig. 4b).

To determine if peripheral B maturation was altered in B6.56R.Aec1/2 mice compared to B6.56R mice, we analyzed splenic B-cell subsets by flow cytometry (Supplementary Fig. S4). These studies revealed that B6.56R mice and B6.56R.Aec1/2 mice had similar peripheral B-cell subset distributions with respect to their transitional B-cell frequency, and both B6.56R and B6.56R.Aec1/2 mice had a relative increase in the marginal zone B-cell population and a relative decrease in the follicular population (Supplementary Fig. S5). Earlier studies documented an increased frequency of marginal zone B cells in B6.Aec1/2 mice compared to B6 (53). We did not observe this, but the mice used in most of our immunophenotyping experiments were between 3 and 6 months of age. It is possible that the marginal zone phenotype is more prominent in older mice.

Even if the B-cell subsets of B6.56R and B6.56R.Aec1/2 mice appear to be similar, it is still possible that there are differences in the selected repertoire between the two strains. For example, the receptor editing defect conferred by Aec1/2 could skew the mature B-cell repertoire towards more autoreactive (and potentially less edited) anti-DNA B cells. To determine if receptor edited B cells are less frequent among mature B cells of B6.56R.Aec1/2 mice compared to B6.56R mice, we analyzed the antibody heavy chain allotype usage. In B6.56R mice, the anti-DNA heavy chain knock-in (56R) expresses the IgM(a) allotype, whereas the endogenous heavy chain allele expresses the IgM(b) allotype. If a 56R B cell undergoes heavy chain editing, it is more likely to express the IgM(b) allotype (37, 48). Therefore, we compared the frequency of IgM(b) usage in splenic B cells of B6.56R and B6.56R.Aec1/2. We observed a decreased frequency of IgM(b) on the Aec1/2 background (Fig. 4c). The reduced frequency of IgM(b) usage in B6.56R.Aec1/2 compared to B6.56R mice is consistent with a decreased frequency of receptor editing and, potentially, relaxation of B-cell selection.

To test the functional consequences of this shift in the antibody repertoire more directly, we compared serum autoantibody levels in B6.56R and B6.56R.Aec1/2 mice. B6.56R.Aec1/2 mice had lower levels of serum IgM than B6.56R mice (Supplementary Fig. S6a), but similar levels of IgA and IgG (Supplementary Figs. S6b-S6c), even when mice were stratified by age (Supplementary Fig. S6d). When serum IgG anti-chromatin antibodies were analyzed, the levels were comparable in B6.56R and B6.56R.Aec1/2 (Supplementary Figs. S7a, S7b). Serum anti-dsDNA antibodies were similar for IgM and lower for IgG and IgA in B6.56R.Aec1/2 mice than in B6.56R mice (Supplementary Fig. S7c, S7d and S7e).

B6.56R.Aec1/2 mice have less severe disease than B6.Aec1/2 mice

We were surprised that serum anti-DNA antibody titers were lower in B6.56R.Aec1/2 mice than in B6.56R mice and wondered if the decrease on the Aec1/2 background reflected sequestration of autoreactive B cells and their antibodies in the salivary glands. If such sequestration were occurring, we reasoned that salivary gland histology should reveal more severe lymphocytic infiltration in B6.56R.Aec1/2 mice than in B6.56R mice. Consistent with previously published findings (63), we observed an age-dependent increase in salivary

gland infiltration in B6.Aec1/2 mice (Supplementary Fig. S8). We also noted that the submandibular gland of B6.Aec1/2 mice is the most frequently affected gland (data not shown). The histology of the tubular epithelia in the submandibular gland differs in male and female mice (64), but lymphocytic infiltrations can be found in either histologic variant (Fig. 5a). Consistent with previously published findings (ref. 50), the infiltrates include B cells and T cells (Fig. 5b). The degree of lymphocytic infiltration was quantified by measuring the number of lymphocytic infiltrates in a defined area of tissue, producing a focus score (described further in the *Methods* section). We observed that B6.Aec1/2 mice had higher focus scores than B6.56R.Aec1/2 mice, which is the opposite of what we had expected to find if there had been glandular sequestration of pathogenic autoantibodies (Fig. 5c). Furthermore, we noticed that older B6 mice and B6.56R mice (>12 months of age) also exhibited salivary gland pathology (Fig. 5d). Thus, on either the B6 or the B6.Aec1/2 background, the presence of the 56R transgene appeared to have a protective effect: B6.56R mice had fewer salivary gland infiltrates than B6 mice and similarly, B6.56R.Aec1/2 mice had fewer salivary gland infiltrates than B6.Aec1/2 mice. We did not observe any correlation between the serum autoantibody levels and salivary gland inflitration for anti-chromatin or anti-dsDNA in either B6.56R or B6.56R.Aec1/2 (data not shown). We also did not observe a significant difference in the frequency or size of lymphocytic infiltrations in the kidneys of B6.Aec1/2 (n=14), B6.56R.Aec1/2 (n=16), B6 (n=6 mice) or B6.56R (n=10) controls (data not shown).

Discussion

The B6.Aec1/2 mouse model exhibits several signs of SjS including age and sex-dependent lymphocytic infiltration of the salivary and lacrimal glands, reduced tear production and the presence of serum autoantibodies (31). Despite the clinical phenotype, the B-cell abnormalities in these mice, particularly in the younger animals, seem comparatively mild. There are slight decreases in the proportion of pre-B cells in the bone marrow and correspondingly lower frequencies of receptor editing. Peripherally, there is an expansion of recirculating B cells. Serum immunoglobulin levels are normal or slightly decreased compared to B6 mice, and serum autoantibody profiles reveal subtle changes compared to age-matched control strains.

In an effort to exacerbate the disease effects of these alterations in B-cell development and receptor editing, the B6.Aec1/2 mouse was crossed onto an anti-dsDNA heavy chain knock-in strain called B6.56R. B cells in B6.56R mice undergo extensive antibody light chain receptor editing in order to minimize DNA binding of the 56R heavy chain (35). We therefore expected that the B6.Aec1/2 mouse, with its receptor editing defect, to exhibit more severe disease and higher titers of anti-DNA autoantibodies. Neither of these expected outcomes was observed. Instead, the 56R transgene appeared to have a protective effect: B6.56R.Aec1/2 mice had less severe sialadenitis than B6.Aec1/2 mice, and dsDNA antibody titers were similar or slightly lower in B6.56R.Aec1/2 mice than in B6.56R mice. Remarkably, a similar effect was observed when older (>12 months) B6 and B6.56R mice were compared, with B6 mice having more sialadenitis than B6.56R mice, despite the higher levels of anti-DNA and anti-chromatin antibodies in the B6.56R mouse.

The extent of sialadenitis was not correlated with the levels of serum autoantibodies to dsDNA or chromatin. However, one of the most consistent changes we observed was a *reduction* in serum IgA levels on the B6.Aec1/2 background. It is possible that IgA secreting B cells are sequestered in the mucosa associated lymphoid tissue (MALT). In this connection, it is intriguing that patients with SjS are at increased risk for MALT lymphomas, including those that arise in the salivary glands themselves (65, 66). Intriguingly, low serum IgA levels have also been described in association with non-

Hodgkin's B-cell lymphomas (67). IgA levels could be down-regulated in the setting of lymphoma (a phenomenon termed immune paresis) or individuals with lower IgA levels could be at increased risk of developing lymphoma. It is also possible that IgA has a negative immunomodulatory role and that lower serum IgA levels reflect a state of immune dysregulation in SjS and other autoimmune conditions. In this connection, it is noteworthy that individuals with selective IgA deficiency have higher frequencies of several autoimmune susceptibility loci, although the mechanistic basis for this association remains to be explained (68).

Our data also indicate that sialadenitis in older mice appears to occur in all four strains of mice that were analyzed (B6, B6.Aec1/2, B6.56R and B6.56R.Aec1/2). The levels of sialoadenitis were not significantly higher in mice carrying the Aec1/2 genetic intervals. The presence of sialoadenitis in older B6 mice indicates that the B6 genetic background is autoimmune-prone, consistent with previously published findings by Hayashi and colleagues (69). Thus the attribution of autoimmune phenotypes requires caution and consideration of the genetic background, particularly in older animals. Another caveat to this work is that during the course of this study some of the older homozygous B6.Aec1/2 mice died, so it is possible that the histology of older B6.Aec1/2 mice seems less severe due to undersampling of the most severely affected (dead) animals.

Perhaps the most surprising observation was that the receptor editing defect in B6.Aec1/2 mice did not appear to cause significant problems when B6.56R was crossed onto the B6.Aec1/2 strain. The receptor editing defect in B6.Aec1/2 may be mild enough that peripheral B-cell tolerance mechanisms can compensate for the editing defect. Another possibility is that the editing defect in B6.Aec1/2 mice is significant, but that its effects on the 56R transgene are insufficient to limit autoreactivity, even in wild type mice. Indeed, B6.56R and even B6 mice spontaneously break tolerance to dsDNA, so clearly editing is not a panacea (49, 61, 70). Even when antibody light chains are edited in B6.56R mice, most do not fully negate the autoreactive specificity of the 56R heavy chain. Some editing rearrangements result in allelic inclusion (71). B cells that co-express kappa and lambda light chains can produce a mixture of self and non-self-reactive antibodies and can be found in the marginal zone of anti-DNA mice (72). Furthermore, receptor editing of heavy chains, for example by V_H replacement, can increase the CDR3 length without eliminating most of the original CDR3 (48). There is a highly conserved arginine residue at the 3′ end of most V_H genes, thus V_H replacement can increase the arginine content of the CDR3. CDR3 is in the center of the antigen binding site, and elongated CDR3s are associated with multireactive or frankly autoreactive antibody specificities (73).

As the disease phenotype in B6.56R.Aec1/2 mice appears to be less severe than in B6.Aec1/2 mice, it seems likely that the receptor editing defect is, in and of itself, insufficient to cause clinical disease: rather, a "second hit" may be required. That second hit could consist of the right autoantibody specificity in the right environment. How and why particular autoantibody specificities are propagated in specific autoimmune diseases remains a fundamental mystery in autoimmunity. Perhaps only in the setting of a diverse B-cell (and T-cell) repertoire is it likely for one or more critical autospecificities to emerge. The observation that diversity of the antigen receptor contributes to autoimmunity has been demonstrated in TdT knock-out mice. TdT knockout mice have greatly reduced antibody heavy chain junctional diversity (due to the absence of N-addition) and have a less severe disease phenotype when crossed onto the autoimmune-prone B6.lpr strain (74). In a similar vein, the imposition of a TCR transgene on the B6.lpr strain appears to have beneficial effects, including reduced lymphadenopathy, even when that transgene recognizes a self antigen (75). Perhaps the 56R autoantibody is the wrong autoantibody for the B6.Aec1/2 salivary gland microenvironment. The lack of B-cell clones of a particular autospecificity

may limit T-B collaboration and disease propagation. It is still unclear from these data if the B-cell defects cause or arise as a consequence of other immunologic perturbations in the B6.Aec1/2 strain. Nevertheless, these findings suggest that therapies that reduce B-cell numbers or diversity could be beneficial in SjS.

Conclusions

The B-cell defects in the B6.Aec1/2 mouse model of Sjögren's syndrome are mild, but do include an early B-cell checkpoint defect with reduced receptor editing and altered early B-cell development. Breeding the Aec1/2 genetic intervals onto the B6.56R anti-dsDNA knock-in model (in which receptor editing is extensively relied upon to reduce the production of anti-dsDNA antibodies) did *not* result in an exacerbation of disease. Instead, if anything, B6.56R.Aec1/2 mice appeared to fare better than B6.Aec1/2 or B6.56R mice, producing similar or lower levels of autoantibodies and exhibiting less sialoadenitis. These data suggest that the early tolerance checkpoint defect in B6.Aec1/2 mice is not sufficient to promulgate disease in mice with pre-formed autoantibodies, such as B6.56R. Rather, B6.Aec1/2 mice may require a diverse B-cell repertoire for efficient T-B-cell collaboration and disease propagation. These findings imply that therapies aimed at reducing B-cell diversity or T-B interactions may be helpful in treating SjS.

Supplementary Material

Refer to Web version on PubMed Central for supplementary material.

Acknowledgments

This work was supported by NIH grants R01 DE017590, R01 AR34156 and R01 AI063626, the Sjögren's syndrome Foundation the Lupus Research Institute, the Alliance for Lupus Research, the Arthritis Foundation and the American Autoimmunity Related Disease Association. We thank Patricia Y. Tsao for help with the ELISAs and Tianying Jiang for help with histology and imaging and Siyuan Hu for help with digital figures. We also thank the University of Pennsylvania flow cytometry core facility, histology core and the molecular genotyping facilities at the Hospital of the University of Pennsylvania (Department of Pathology and Laboratory Medicine) and the Department of Genetics core laboratory at the University of Pennsylvania for skilled technical assistance.

Abbreviations

SjS	Sjögren's syndrome
V_H	antibody H chain variable region gene
Fr. B-C	bone marrow pro-B cells
Fr.C′	bone marrow cycling pre-B cells
Fr. D	bone marrow pre-B cells
RS deletion	kappa light chain deletional rearrangements
IgH	immunoglobulin heavy chain
IgL	immunoglobulin light chain
ANA	anti-nuclear antibody

References

1. Tan EM. Autoantibodies to nuclear antigens (ANA): their immunobiology and medicine. Adv Immunol. 1982; 33:167–240. [PubMed: 6182766]

2. Franceschini F, Cavazzana I. Anti-Ro/SSA and La/SSB antibodies. Autoimmunity. 2005; 38(1):55–63. [PubMed: 15804706]
3. Cha S, Singson E, Cornelius J, Yagna JP, Knot HJ, Peck AB. Muscarinic acetylcholine type-3 receptor desensitization due to chronic exposure to Sjogren's syndrome-associated autoantibodies. J Rheumatol. 2006; 33(2):296–306. [PubMed: 16465661]
4. Gao J, Cha S, Jonsson R, Opalko J, Peck AB. Detection of anti-type 3 muscarinic acetylcholine receptor autoantibodies in the sera of Sjogren's syndrome patients by use of a transfected cell line assay. Arthritis Rheum. 2004; 50(8):2615–21. [PubMed: 15334476]
5. Peen E, Mellbye OJ, Haga HJ. IgA rheumatoid factor in primary Sjogren's syndrome. Scand J Rheumatol. 2009; 38(1):46–9. [PubMed: 18942022]
6. Muller K, Oxholm P, Mier-Madsen M, Wiik A. Circulating IgA- and IgM-rheumatoid factors in patients with primary Sjogren syndrome. Correlation to extraglandular manifestations. Scand J Rheumatol. 1989; 18(1):29–31. [PubMed: 2784865]
7. Gondran G, Fauchais A, Lambert M, Ly K, Launay D, Queyrel V, et al. Primary Sjogren's syndrome in men. Scand J Rheumatol. 2008; 37(4):300–5. [PubMed: 18612931]
8. Vissink A, Kallenberg CG, Bootsma H. Treatment approaches in primary Sjogren syndrome. Jama. 304(18):2015–6. author reply 2016. [PubMed: 21063008]
9. Delaleu N, Jonsson R, Koller MM. Sjogren's syndrome. European journal of oral sciences. 2005; 113(2):101–113. [PubMed: 15819815]
10. Christodoulou MI, Kapsogeorgou EK, Moutsopoulos HM. Characteristics of the minor salivary gland infiltrates in Sjogren's syndrome. J Autoimmun. 2010; 34(4):400–7. [PubMed: 19889514]
11. Brookes SM, Cohen SB, Price EJ, Webb LM, Feldmann M, Maini RN, et al. T cell clones from a Sjogren's syndrome salivary gland biopsy produce high levels of IL-10. Clin Exp Immunol. 1996; 103(2):268–72. [PubMed: 8565310]
12. Coll J, Gambus G, Corominas J, Tomas S, Esteban JI, Guardia J. Immunohistochemistry of minor salivary gland biopsy specimens from patients with Sjogren's syndrome with and without hepatitis C virus infection. Ann Rheum Dis. 1997; 56(6):390–2. [PubMed: 9227171]
13. Kasna-Ronkainen LT. Sjogren's syndrome: viewpoint on pathogenesis. Scandinavian Journal of Rheumatology. 2002; 31:15. [PubMed: 12109538]
14. Hansen A, Lipsky PE, Dorner T. B cells in Sjogren's syndrome: indications for disturbed selection and differentiation in ectopic lymphoid tissue. Arthritis Res Ther. 2007; 9(4):218. [PubMed: 17697366]
15. Nguyen CQ, Cha SR, Peck AB. Sjogren's syndrome (SjS)-like disease of mice: the importance of B lymphocytes and autoantibodies. Front Biosci. 2007; 12:1767–89. [PubMed: 17127420]
16. Pablos JL, Carreira PE, Morillas L, Montalvo G, Ballestin C, Gomez-Reino JJ. Clonally expanded lymphocytes in the minor salivary glands of Sjogren's syndrome patients without lymphoproliferative disease. Arthritis Rheum. 1994; 37(10):1441–4. [PubMed: 7945468]
17. Tzioufas AG. B-cell lymphoproliferation in primary Sjogren's syndrome. Clin Exp Rheumatol. 1996; 14 (Suppl 14):S65–70. [PubMed: 8722203]
18. Harris NL. Lymphoid proliferations of the salivary glands. Am J Clin Pathol. 1999; 111(1 Suppl 1):S94–103. [PubMed: 9894474]
19. Hansen A, Lipsky PE, Dorner T. B-cell lymphoproliferation in chronic inflammatory rheumatic diseases. Nat Clin Pract Rheumatol. 2007; 3(10):561–9. [PubMed: 17906611]
20. Mariette X, Roux S, Zhang J, Bengoufa D, Lavie F, Zhou T, et al. The level of BLyS (BAFF) correlates with the titre of autoantibodies in human Sjogren's syndrome. Ann Rheum Dis. 2003; 62(2):168–71. [PubMed: 12525388]
21. Groom J, Kalled SL, Cutler AH, Olson C, Woodcock SA, Schneider P, et al. Association of BAFF/BLyS overexpression and altered B cell differentiation with Sjogren's syndrome. J Clin Invest. 2002; 109(1):59–68. [PubMed: 11781351]
22. Bunim JJ. The frequent occurrence of hypergammaglobulinemia and multiple tissue antibodies in Sjogren's syndrome. Ann N Y Acad Sci. 1965; 124(2):852–9. [PubMed: 4158449]
23. Kassan SS, Thomas TL, Moutsopoulos HM, Hoover R, Kimberly RP, Budman DR, et al. Increased risk of lymphoma in sicca syndrome. Ann Intern Med. 1978; 89(6):888–92. [PubMed: 102228]

24. Voulgarelis M, Dafni UG, Isenberg DA, Moutsopoulos HM. Malignant lymphoma in primary Sjogren's syndrome: a multicenter, retrospective, clinical study by the European Concerted Action on Sjogren's Syndrome. Arthritis Rheum. 1999; 42(8):1765–72. [PubMed: 10446879]
25. Henriksson G, Sallmyr A, Du L, Larsson A, Manthorpe R, Bredberg A. Enhanced DNA-dependent protein kinase activity in Sjogren's syndrome B cells. Rheumatology (Oxford). 2004; 43(9):1109–15. [PubMed: 15213331]
26. Hansen A, Gosemann M, Pruss A, Reiter K, Ruzickova S, Lipsky PE, et al. Abnormalities in peripheral B cell memory of patients with primary Sjogren's syndrome. Arthritis Rheum. 2004; 50(6):1897–908. [PubMed: 15188366]
27. Bohnhorst JO, Bjorgan MB, Thoen JE, Natvig JB, Thompson KM. Bm1-Bm5 classification of peripheral blood B cells reveals circulating germinal center founder cells in healthy individuals and disturbance in the B cell subpopulations in patients with primary Sjogren's syndrome. Journal of Immunology. 2001; 167(7):3610–8.
28. Humphreys-Beher MG, Peck AB. New concepts for the development of autoimmune exocrinopathy derived from studies with the NOD mouse model. Arch Oral Biol. 1999; 44 (Suppl 1):S21–5. [PubMed: 10414851]
29. Christopher PR, Shigeo Y, Denise IB, Jason B, Roland J, Rikard H, et al. A novel NOD-derived murine model of primary Sjögren's syndrome. Arthritis and Rheumatism. 1998; 41(1):150–156. [PubMed: 9433880]
30. Brayer J, Lowry J, Cha S, Robinson CP, Yamachika S, Peck AB, et al. Alleles from chromosomes 1 and 3 of NOD mice combine to influence Sjögren's syndrome-like autoimmune exocrinopathy. The Journal of rheumatology. 2000; 27(8):1896–1904. [PubMed: 10955330]
31. Cha S, Nagashima H, Brown VB, Peck AB, Humphreys-Beher MG. Two NOD *Idd*-associated intervals contribute synergistically to the development of autoimmune exocrinopathy (Sjoren's syndrome) on a healthy murine background. Arthritis and Rheumatism. 2002; 46(5):1390–1398. [PubMed: 12115247]
32. Johnston CM, Wood AL, Bolland DJ, Corcoran AE. Complete Sequence Assembly and Characterization of the C57BL/6 Mouse Ig Heavy Chain V Region. Journal of Immunology. 2006; 176(7):4221–4234.
33. Thiebe R, Schable KF, Bensch A, Brensing-Kuppers J, Heim V, Kirschbaum T, et al. The variable genes and gene families of the mouse immunoglobulin kappa locus. Eur J Immunol. 1999; 29(7): 2072–81. [PubMed: 10427969]
34. Brekke KM, Garrard WT. Assembly and analysis of the mouse immunoglobulin kappa gene sequence. Immunogenetics. 2004; 56(7):490–505. [PubMed: 15378297]
35. Li H, Jiang Y, Prak EL, Radic M, Weigert M. Editors and Editing of Anti-DNA Receptors. Immunity. 2001; 15(6):947–957. [PubMed: 11754816]
36. Sekiguchi DR, Yunk L, Gary D, Charan D, Srivastava B, Allman D, et al. Development and Selection of Edited B Cells in B6.56R Mice. Journal of Immunology. 2006; 176(11):6879–6887.
37. Liu Y, Li L, Kumar KR, Xie C, Lightfoot S, Zhou XJ, et al. Lupus Susceptibility Genes May Breach Tolerance to DNA by Impairing Receptor Editing of Nuclear Antigen-Reactive B Cells. Journal of Immunology. 2007; 179(2):1340–1352.
38. Khan SN, Witsch EJ, Goodman NG, Panigrahi AK, Chen C, Jiang Y, et al. Editing and escape from editing in anti-DNA B cells. Proceedings of the National Academy of Sciences of the United States of America. 2008; 105(10):3861–3866. [PubMed: 18310318]
39. Erikson J, Radic MZ, Camper SA, Hardy RR, Carmack C, Weigert M. Expression of anti-DNA immunoglobulin transgenes in non-autoimmune mice. Nature. 1991; 349(6307):331–4. [PubMed: 1898987]
40. Chen C, Nagy Z, Luning Prak E, Weigert M. Immunoglobulin Heavy Chain Gene Replacement: A Mechanism of Receptor Editing. Immunity. 1995; 3(6):747–756. [PubMed: 8777720]
41. Yui MA, Muralidharan K, Moreno-Altamirano B, Perrin G, Chestnut K, Wakeland EK. Production of congenic mouse strains carrying NOD-derived diabetogenic genetic intervals: an approach for the genetic dissection of complex traits. Mamm Genome. 1996; 7(5):331–4. [PubMed: 8661724]

42. Hardy RR, Carmack CE, Shinton SA, Kemp JD, Hayakawa K. Resolution and characterization of pro-B and pre-pro-B cell stages in normal mouse bone marrow. J Exp Med. 1991; 173(5):1213–1225. [PubMed: 1827140]
43. Segerberg-Konttinen M, Konttinen YT, Bergroth V. Focus score in the diagnosis of Sjogren's syndrome. Scand J Rheumatol Suppl. 1986; 61:47–51. [PubMed: 3473649]
44. Rahman ZS, Shao WH, Khan TN, Zhen Y, Cohen PL. Impaired apoptotic cell clearance in the germinal center by Mer-deficient tingible body macrophages leads to enhanced antibody-forming cell and germinal center responses. Journal of Immunology. 2010; 185(10):5859–68.
45. Schlissel MS, Baltimore D. Activation of immunoglobulin kappa gene rearrangement correlates with induction of germline kappa gene transcription. Cell. 1989; 58(5):1001–7. [PubMed: 2505932]
46. Prak EL, Trounstine M, Huszar D, Weigert M. Light chain editing in kappa-deficient animals: a potential mechanism of B cell tolerance. J Exp Med. 1994; 180(5):1805–15. [PubMed: 7964462]
47. Meng W, Yunk L, Wang LS, Maganty A, Xue E, Cohen PL, et al. Selection of Individual VH Genes Occurs at the Pro-B to Pre-B Cell Transition. Journal of Immunology. 2011; 187(4):1835–44.
48. Yunk L, Meng W, Cohen PL, Eisenberg RA, Luning Prak ET. Antibodies in a Heavy Chain Knock-In Mouse Exhibit Characteristics of Early Heavy Chain Rearrangement. Journal of immunology. 2009; 183(1):452–461.
49. Tsao PY, Jiao J, Ji MQ, Cohen PL, Eisenberg RA. T cell-independent spontaneous loss of tolerance by anti-double-stranded DNA B cells in C57BL/6 mice. Journal of Immunology. 2008; 181(11):7770–7.
50. Li Y, Chen F, Putt M, Koo YK, Madaio M, Cambier JC, et al. B cell depletion with anti-CD79 mAbs ameliorates autoimmune disease in MRL/lpr mice. Journal of Immunology. 2008; 181(5): 2961–72.
51. Satoh M, Langdon JJ, Hamilton KJ, Richards HB, Panka D, Eisenberg RA, et al. Distinctive immune response patterns of human and murine autoimmune sera to U1 small nuclear ribonucleoprotein C protein. J Clin Invest. 1996; 97(11):2619–26. [PubMed: 8647956]
52. Satoh M, Reeves WH. Induction of lupus-associated autoantibodies in BALB/c mice by intraperitoneal injection of pristane. J Exp Med. 1994; 180(6):2341–6. [PubMed: 7964507]
53. Nguyen CQ, Kim H, Cornelius JG, Peck AB. Development of Sjogren's syndrome in nonobese diabetic-derived autoimmune-prone C57BL/6. NOD-Aec1Aec2 mice is dependent on complement component-3. Journal of Immunology. 2007; 179(4):2318–29.
54. Delaleu N, Nguyen CQ, Peck AB, Jonsson R. Sjogren's syndrome: studying the disease in mice. Arthritis Res Ther. 2011; 13(3):217. [PubMed: 21672284]
55. Nguyen C, Cornelius J, Singson E, Killedar S, Cha S, Peck AB. Role of complement and B lymphocytes in Sjoren's syndrome-like autoimmune exocrinopathy of NOD. B10-H2b mice. Molecular Immunology. 2006; 43(9):1332–1339. [PubMed: 16221495]
56. Oberdoerffer P, Novobrantseva TI, Rajewsky K. Expression of a targeted lambda 1 light chain gene is developmentally regulated and independent of Ig kappa rearrangements. J Exp Med. 2003; 197(9):1165–72. [PubMed: 12719477]
57. Sonoda E, Pewzner-Jung Y, Schwers S, Taki S, Jung S, Eilat D, et al. B cell development under the condition of allelic inclusion. Immunity. 1997; 6(3):225–233. [PubMed: 9075923]
58. Panigrahi AK, Goodman NG, Eisenberg RA, Rickels MR, Naji A, Luning Prak ET. RS rearrangement frequency as a marker of receptor editing in lupus and type 1 diabetes. Journal of Experimental Medicine. 2008; 205(13):2985–2994. [PubMed: 19075293]
59. Moore MW, Durdik J, Persiani DM, Selsing E. Deletions of kappa chain constant region genes in mouse lambda chain-producing B cells involve intrachromosomal DNA recombinations similar to V-J joining. Proc Natl Acad Sci U S A. 1985; 82(18):6211–5. [PubMed: 3929252]
60. Muller B, Stappert H, Reth M. A physical map and analysis of the murine C kappa-RS region show the presence of a conserved element. Eur J Immunol. 1990; 20(6):1409–11. [PubMed: 2115001]
61. Sekiguchi DR, Yunk L, Gary D, Charan D, Srivastava B, Allman D, et al. Development and selection of edited B cells in B6.56R mice. Journal of Immunology. 2006; 176(11):6879–87.

62. Doyle CM, Han J, Weigert MG, Luning Prak ET. Consequences of receptor editing at the lambda locus: multireactivity and light chain secretion. Proc Natl Acad Sci U S A. 2006; 103(30):11264–11269. [PubMed: 16847259]
63. Cha S, Nagashima H, Brown VB, Peck AB, Humphreys-Beher MG. Two NOD Idd-associated intervals contribute synergistically to the development of autoimmune exocrinopathy (Sjogren's syndrome) on a healthy murine background. Arthritis Rheum. 2002; 46(5):1390–8. [PubMed: 12115247]
64. Lacassagne A. Dimorphisme sexual de la glande sous-maxillaire chez la souris. CR Soc Biol (Paris). 1940; 133:180–181.
65. Dias C, Isenberg DA. Susceptibility of patients with rheumatic diseases to B-cell non-Hodgkin lymphoma. Nat Rev Rheumatol. 7(6):360–8. [PubMed: 21637317]
66. Movahed R, Weiss A, Velez I, Dym H. Submandibular gland MALT lymphoma associated with Sjogren's syndrome: case report. J Oral Maxillofac Surg. 69(11):2924–9. [PubMed: 21549473]
67. Datta U, Kaur K, Varma SC, Bhaskar KV, Sehgal S. Secondary immune defects in non-Hodgkin's lymphoma. Indian J Med Res. 1992; 96:91–5. [PubMed: 1428071]
68. Ferreira RC, Pan-Hammarstrom Q, Graham RR, Gateva V, Fontan G, Lee AT, et al. Association of IFIH1 and other autoimmunity risk alleles with selective IgA deficiency. Nat Genet. 42(9):777–80. [PubMed: 20694011]
69. Hayashi, Y.; Utsuyama, M.; Kurashima, C.; Hirokawa, K. Spontaneous development of organ-specific autoimmune lesions in aged C57BL/6 mice. 1989. p. 120-126.
70. Sekiguchi DR, Eisenberg RA, Weigert M. Secondary heavy chain rearrangement: a mechanism for generating anti-double-stranded DNA B cells. J Exp Med. 2003; 197(1):27–39. [PubMed: 12515811]
71. Li Y, Louzoun Y, Weigert M. Editing Anti-DNA B Cells by V{lambda}x. Journal of Experimental Medicine. 2004; 199(3):337–346. [PubMed: 14757741]
72. Li Y, Li H, Weigert M. Autoreactive B cells in the marginal zone that express dual receptors. J Exp Med. 2002; 195(2):181–8. [PubMed: 11805145]
73. Wardemann H, Yurasov S, Schaefer A, Young JW, Meffre E, Nussenzweig MC. Predominant autoantibody production by early human B cell precursors. Science. 2003; 301(5638):1374–7. [PubMed: 12920303]
74. Molano ID, Wloch MK, Alexander AA, Watanabe H, Gilkeson GS. Effect of a Genetic Deficiency of Terminal Deoxynucleotidyl Transferase on Autoantibody Production by C57BL6 Faslpr Mice. Clinical Immunology. 2000; 94(1):24–32. [PubMed: 10607487]
75. Mountz JD, Zhou T, Eldridge J, Berry K, Bluthmann H. Transgenic rearranged T cell receptor gene inhibits lymphadenopathy and accumulation of CD4-CD8-B220+ T cells in lpr/lpr mice. J Exp Med. 1990; 172(6):1805–17. [PubMed: 1701823]

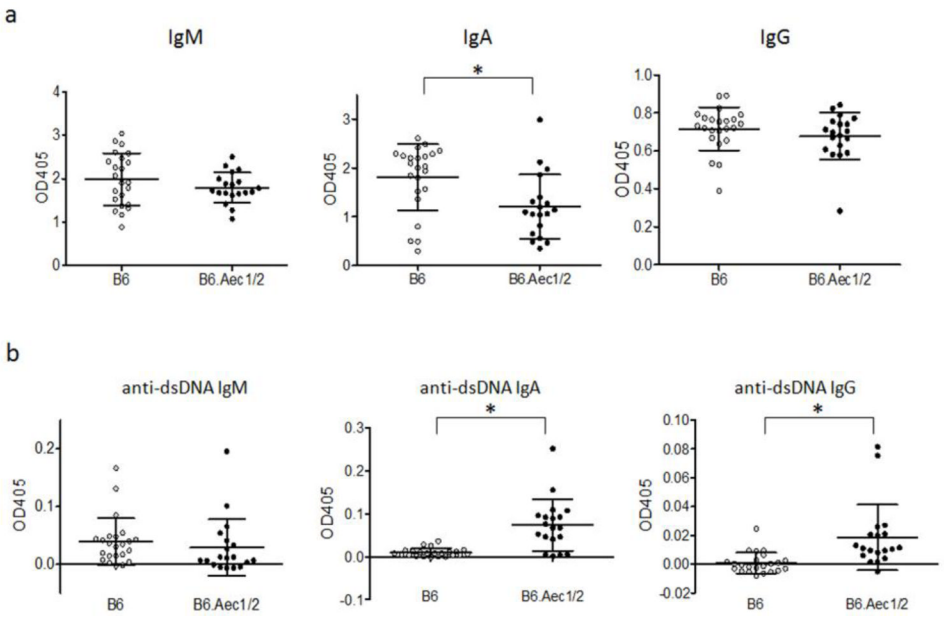

Fig. 1. IgM, IgA and IgG antibody levels and anti-dsDNA antibodies

Sera were obtained from B6 (n=23 females), B6.Aec1/2 (n =19 females) mice that ranged in age from 2 mo to 24 mo. Average OD values (of duplicate readings) for individual mice are indicated (grey symbols indicate B6, black symbols indicate B6.Aec1/2). a. Serum IgM, IgA and IgG levels. b. Serum anti-dsDNA IgM, anti-dsDNA IgA and anti-dsDNA IgG antibody levels. Vertical lines represent the confidence interval for one SD. The central horizontal line indicates the arithmetic mean. Asterisks indicate $p < 0.05$ by two-tailed Mann-Whitney test. All ELISA measurements shown were performed in duplicate in the same assay at the same dilution (see materials and methods) on the same day. The OD_{405} measurements were subtracted from the background value (medium alone). These conditions apply to all mouse serum ELISA studies unless specified otherwise.

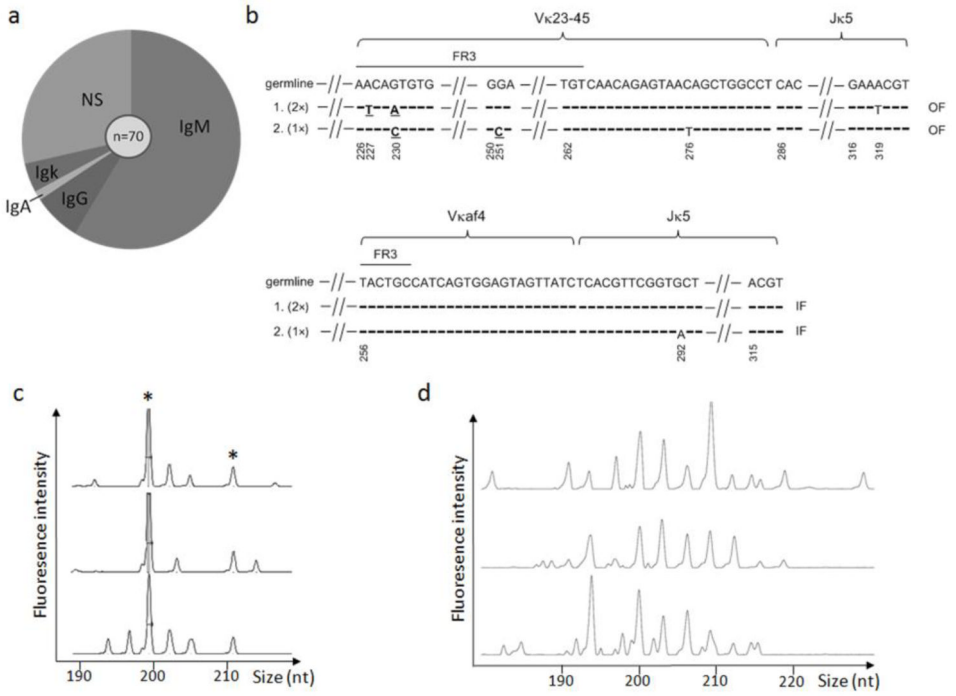

Fig. 2. Spontaneous hybridoma panel analysis

a. 70 hybridomas were generated from a 20-mo-old female B6.Aec1/2 spleen without any stimulation. Among them, 41 expressed IgM, 5 expressed IgG and 1 expressed IgA. Three clones expressed light chain but not IgM, IgG or IgA heavy chains. Twenty clones did not secrete any identifiable heavy chain or light chain (NS = non-secretors). b. Kappa light chain sequencing of clonally related hybridomas. Upper and lower panels represent two expanded clones with the same V**κ**, J**κ** and CDR3 length. The germline V**κ** and J**κ** sequences are shown in the top row for comparison. Horizontal dashes indicate that the nucleotide sequence of the clone is identical to the germline sequence. Sequence changes that result in amino acid replacements are indicated in bold underlined font. Silent mutations are given in regular font. Gaps in the sequence are indicated by angled hatch marks. The sequences in the gap are identical to the germline sequence (not shown). Nucleotide positions are numbered according to their positions in the germline sequences, starting with the V**κ** framework 1 sequence. In the upper group of clonally related hybridomas, two of the three hybridomas (indicated by 2×) have an identical V**κ**-23-J**κ**5 sequence, which has 3 mutations compared to the germline sequences. The third hybridoma (this sequence was recovered only once, 1×) has two mutations compared to the germline sequence. In the lower group of clonally related hybridomas, two of the hybridomas had sequences that were identical to the germline sequence and the third hybridoma had one nucleotide substitution resulting in a silent mutation in J**κ**5. FR3 = framework region 3. IF = in-frame rearrangement (productive). OF = out-of-frame rearrangement (non-productive). c. CDR3 spectratyping of splenocytes from the same B6.Aec1/2 mouse used for hybridoma analysis. J606.1-J_H2 rearrangements were shown from three independent PCRs. Shared peaks in all three independent amplifications (putative clonal expansions) are indicated by the asterisks. d. CDR3 spectratyping of splenocytes from a 23-month-old female B6 mouse. MOPC21-J_H2 rearrangements are shown from three independent PCRs.

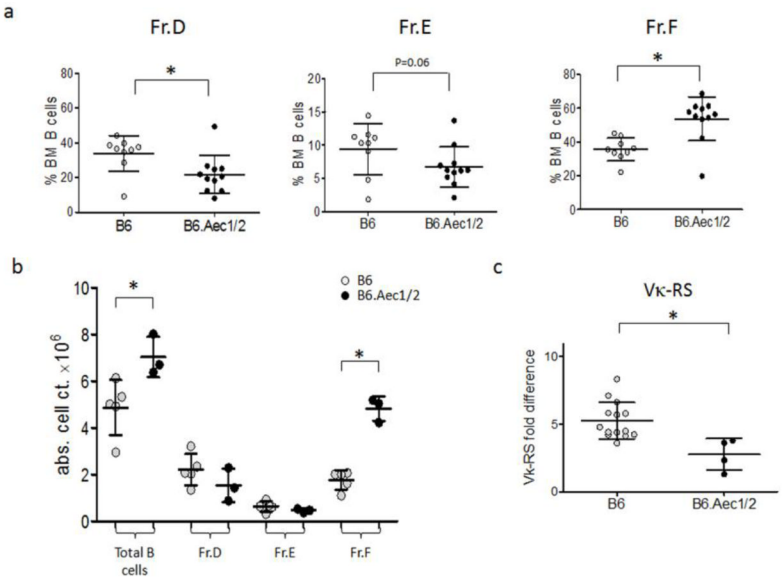

Fig. 3. Bone marrow B-cell subsets and light chain gene rearrangements in B6 and B6.Aec1/2 mice

a. Percentages of bone marrow (% BM) B-cell subsets (Hardy fractions D, E and F as defined in the *Methods*) of B6 (n=9) and B6.Aec1/2 (n=11) mice. Subsets are defined as the fraction of CD19+ BM lymphocytes multiplied by 100%. Asterisks indicate fractions that differ significantly, $p<0.05$ by two-tailed Mann-Whitney test. b. Absolute B-cell numbers of BM fractions of B6.Aec1/2 (n=3) and B6 (n=5) mice. Cell counts were obtained by multiplying the number of viable B220+ BM lymphocytes in each mouse by the percentages of cells in each fraction. Asterisks indicate fractions that differ significantly, $p<0.05$ by two-tailed Mann-Whitney test. c. RS rearrangement frequencies in Fr. D bone marrow B cells from B6 and B6.Aec1/2 mice. The RS frequency is plotted as fold difference relative to kappa+ splenocytes from B6 mice. The average RS frequency is significantly lower in B6.Aec1/2 mice ($p<0.05$ by two-tailed Mann-Whitney test.) In all panels vertical lines represent the confidence interval for one SD. The central horizontal line indicates the arithmetic mean.

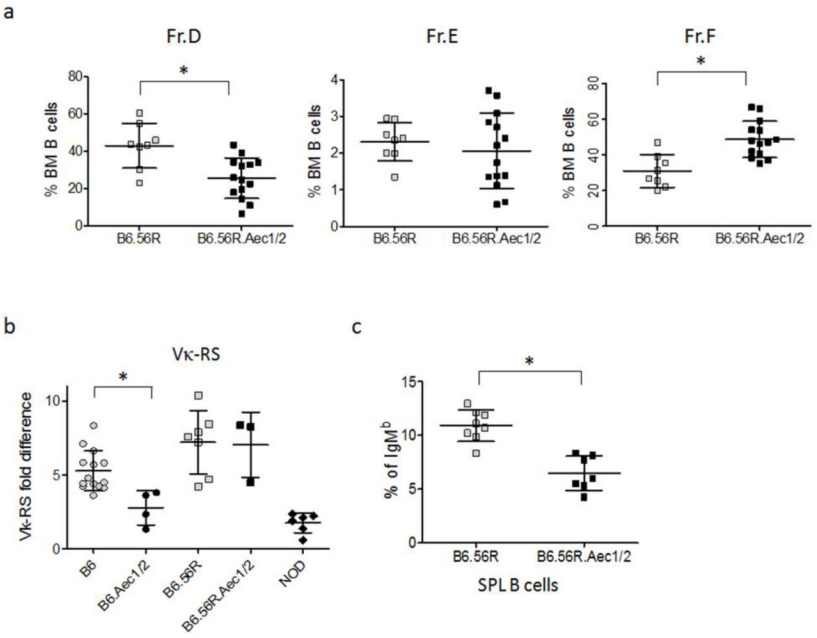

Fig. 4. Comparison of B-cell development and receptor editing in B6.56R and B6.56R.Aec1/2 mice

a. The percentages of bone marrow B cells that comprise fractions D, E and F (as defined in *Methods*) are shown for B6.56R (n=8) and B6.56R.Aec1/2 mice (n=14). b. RS rearrangement frequency in bone marrow fraction D cells from B6 (n = 14, 2–6 mo), B6.Aec1/2 (n=4, 2–14 mo), B6.56R (n=7, 2–6 mo), B6.Aec1/2.56R (n=3, 2–6 mo), and NOD (n=6, 2–6 mo). All PCRs were performed in duplicate. Data are depicted as fold difference relative to the RS level in B6 splenic B220+κ+ B cells. c. Percentages of IgM^b B cells in spenocytes of B6.56R (n=8) and B6.56R.Aec1/2 (n=7).

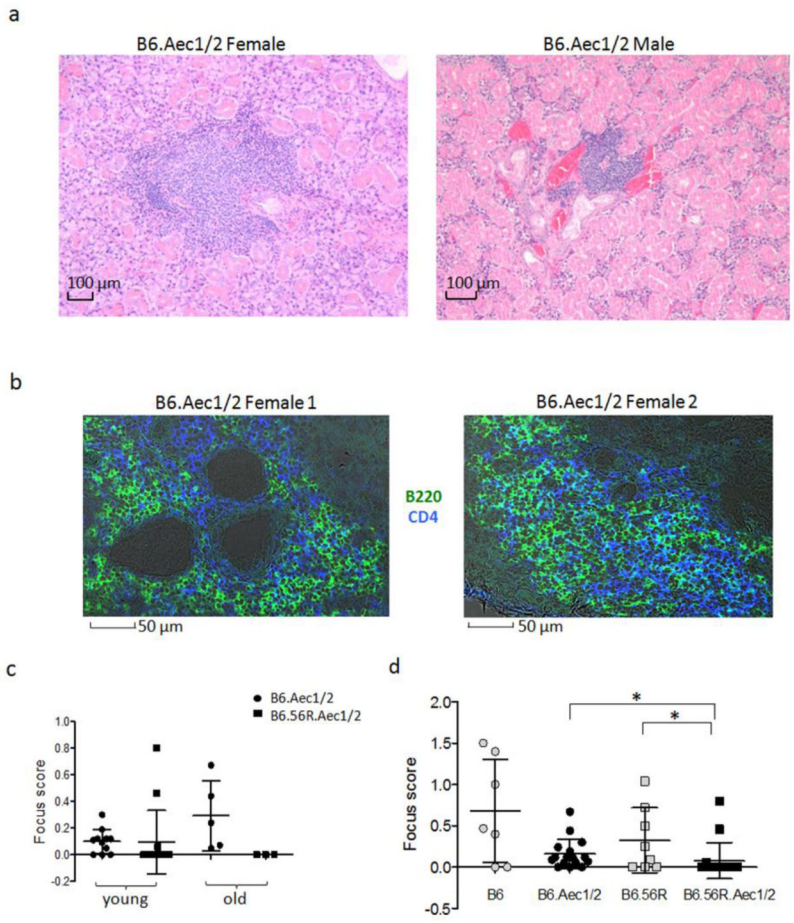

Fig. 5. Lymphocytic infiltration in the salivary glands of B6.Aec1/2 and B6.56R.Aec1/2 mice

a. Lymphocytic infiltrates in the submandibular glands of a female (left panel) and male (right panel) B6.Aec1/2 mouse. Sixteen B6.Aec1/2 mice were evaluated and 14 of them had infiltrates. b. Confocal images of salivary glands in female B6.Aec1/2 mice (n=2, age 6 months) reveal the presence of B cells and CD4 T cells. Green: anti-B220-Alexa488; Blue: anti-CD4-Alexa 647; Grey: phase-contrast image. c. Salivary gland focus score in young (<12 mo) and aged (>12 mo) B6.Aec1/2 (filled circles, young, n=11; old, n=5) and B6.56R.Aec1/2 (filled squares, young, n=14; old, n=3) mice. d. Focus scores of lymphocytic infiltrates in salivary glands of B6 (n=7, n=6 females), B6.Aec (n=16, n=10 females), B6.56R (n=8, n=5 females) and B6.56R.Aec1/2 (n=17, n=7 females). Female ages range from 5- to 25-mo-old, and males range from 6- to 12-mo-old. Asterisks indicate $p < 0.05$ by two-tailed Mann-Whitney test. In panels c and d, vertical lines represent the confidence interval for one SD. The central horizontal line indicates the arithmetic mean.

Table 1

Shown are the reactivity profiles and antibody heavy chain isotype usage for spontaneous hybridomas generated from an old B6.Aec1/2 mouse with serum autoantibodies. The left three columns indicate the reactivity pattern. Each row of the table summarizes all of the clones with a given reactivity profile, starting in the top row with the most polyreactive (those that bind all three autoantigens) and ending with the non-reactive clones (bottom row). The numbers in the columns on the right refer to the number of hybridomas with the indicated reactivity profile that have a given heavy chain isotype. Thus, in the case of the top row, there are three hybridoma supernatants that bind to all three antigens, two of which are IgM antibodies and one of which is an IgA antibody. Positive binding (+) was arbitrarily defined as 2-fold higher than the mean of the OD values for all of the hybridomas.

Reactivity Profile			Heavy chain usage		
dsDNA	Insulin	LPS	IgM	IgG	IgA
+	+	+	2		1
	+	+	8		
+			2	1	
	+		1		
		+	3		
			25	4	